Original Research Article

Resilience in the Face of Seismic Challenges: Design of Earthquake-Resistant Tunnel Supports

Abstract

This paper presents the design of an earthquake-resistant support system in a Himalayan tunnel. A 2D plane strain pseudo-static model employing finite element analysis has been used to assess the seismic performance of the supports after they have been obtained using the Q and RMR approaches. It was found that empirical approaches frequently overestimate or underestimate the support elements when seismic and static loads are used together. This has shown that the best way for the selection of earthquake-resistant supports is by using support capacity plots from finite-element analysis because it helps optimize the required supports. With the help of numerical modeling, a set of safe and optimal supports has been designed for each rock class present in the study area that meets the seismic resistance criteria.

Keywords: Seismic activity; tunnel support; earthquake resistance; geological settings; numerical modeling.

1 INTRODUCTION

Nepal's past is etched with a chronicle of earthquakes with significant magnitudes, weaving a story of its resilience amidst the tremulous ground beneath its feet. The booming construction industry is making constant efforts to consider economic and seismic safety concerns, with tunnel support design and construction being one of the thriving and challenging sectors at the same time. According to information provided during the Nepal Tunneling Conference in 2019, 220 km of tunnel have been completed, while another 195 km are now being built as part of numerous active hydropower construction projects in Nepal [1].

Constructions underground have historically fared better than those on the surface [2]. This is because the soil and rock in the area impede the mobility of subsurface structures. The degree of redundancy of underground structures is greater than that of surface structures because underground structures are supported by the ground while surface structures are frequently unsupported above the ground [3]. Additionally, the increased modulus of elasticity with depth, the smaller excavation dimension relative to the much longer seismic wave length, and the reduction in ground motion amplitude with depth all contribute to the greater seismic resistance of underground structures [4].

Although tunnels are typically considered to be more resistant to seismic damage, numerous instances of such damage have been documented. Notable examples include the 1906 San Francisco earthquake (Mw 7.9), the 1923 Great Kanto earthquake (Mw 7.9-8.2), and the 2008 Wenchuan earthquake (Mw 7.9), which all caused significant harm to mountain tunnels [5]. In the aftermath of the 2015 Gorkha earthquake (Mw 7.8) in Nepal, the Melamchi water supply project tunnel experienced cracks on its inside surface, wall, and crown [6], while Bhairabkunda Hydroelectric Project, Sindhupalchowk reported shotcrete cracking [7]. Such case histories demonstrate the crucial importance of incorporating seismic load considerations into the design of tunnel supports.

This study's main goal is to create tunnel support systems that can survive seismic activity in various geological environments. Squeezing has also been the subject of a thorough investigation over several parts.

2 METHODOLOGY

The goal of this research was to create tunnel support systems that could withstand earthquakes in a variety of geological settings. This was accomplished through a series of consecutive tasks, including a review of the literature on earthquake damage and tunnel support design techniques. Data was gathered for a case study from a variety of sources, including theses, fieldwork, published articles, and lab work. After classifying the rock and soil, empirical techniques like Q and RMR were utilized to evaluate tunnel support. Following the calculation of the rock mass parameters, the tunnel's squeezing study was carried out. Tunnel support study was carried out utilizing Phase 2.0, a finite element modeling software. Finally, for every tunnel-related geological condition, an earthquake-resistant support was chosen. With the help of this thorough methodology, it was possible to create tunnel support systems that can survive seismic activity in a variety of geological settings. Figure 1 shows the flowchart of the methodology adopted for this study.

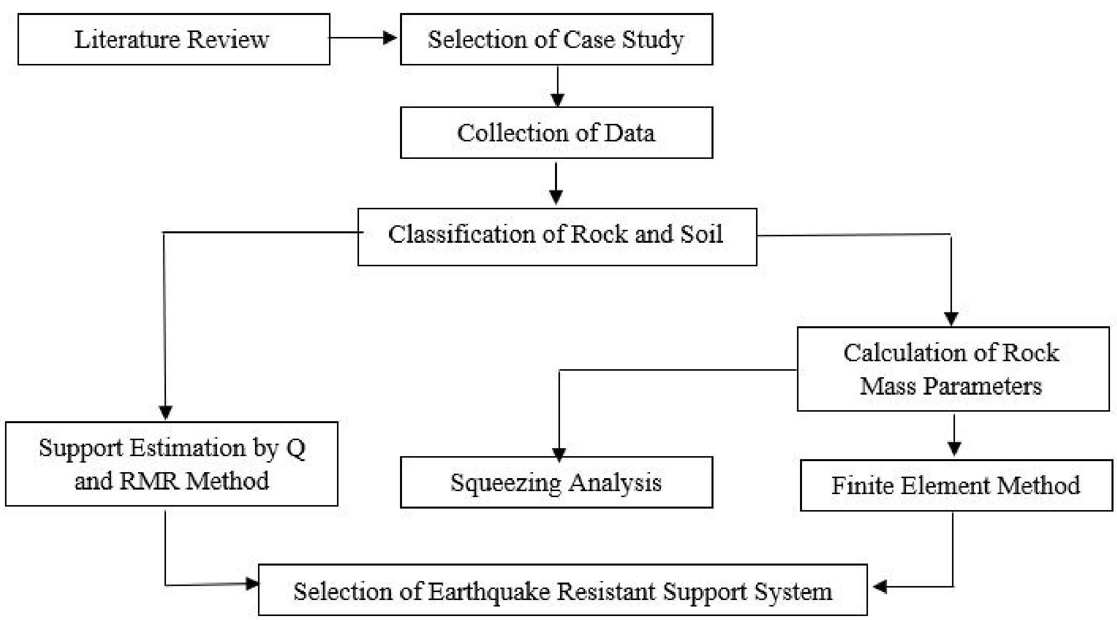

Figure 1: Methodology flowchart

3 PROJECT AREA

Super Madi Hydro Electric Project (44 MW) is a run-of-river type hydropower located in Madi Rural Municipality of Gandaki Province, Nepal. The headrace tunnel is an inverted D-shaped with a diameter of 4.2 m and carries design discharge of 18 m^3/s.

3.1 Geological Description

The SMHEP headrace tunnel is located in Nepal's Lesser Himalayan region, which is south of the Great Himalayas and north of the Siwalik Range. About 2 km (in an aerial distance) to the south of the powerhouse region is where the Main Central Thrust (MCT) is located [8]. Banded gneiss is the main kind of rock present in the area. Figure 2 shows the lithology of the tunnel's longitudinal section.

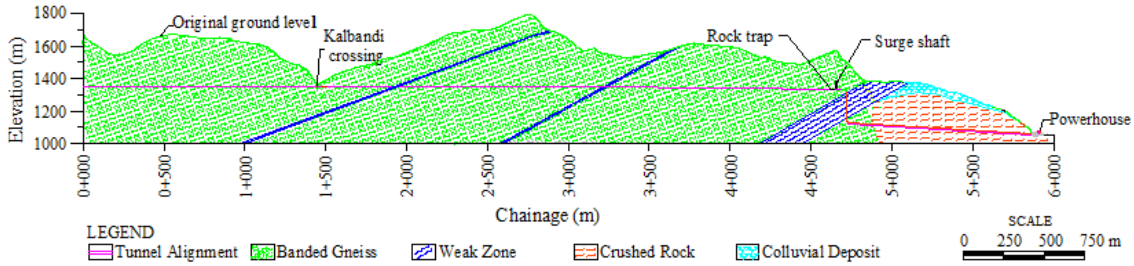

Figure 2: Longitudinal cross-section along the tunnel alignment

3.2 Study section 1

This section comprises of chainages ranging from 1+000 m to 1+500 m and 3+600 m to 3+800 m. It consists of moderately weathered, fresh, medium-strong, foliated, grey-colored, medium-grained, banded gneiss. Quartz veins parallel to the foliation plane are present, while some are folded in section 3+600 m to 3+800 m. Most of the rough, planar, freshly to moderately weathered joints have clay-filled apertures. The joints are closely to moderately spaced and have medium to high persistency, with fair RQD. The rock's Q values range from 0.04 (representing extremely poor rock) to 1.3 (representing poor rock). The RMR values indicate the presence of Fair Rock (41-60) and Poor Rock (21-40).

3.3 Study section 2

The segment between chainage 5+539 m and 5+547 m comprises of heavily disintegrated gneiss, which is severely weathered and has transformed almost completely into residual soil. The soil's matrix is composed of a medium to coarse-grained, silty clay, with a reddish-yellow to brownish color, and boulders are present on both faces and walls. The rock mass has a Q value of 0.00416, which indicates an exceptionally poor rock condition. This section has been numerically modeled as soil for support analysis. Based on the laboratory testing results on soil samples, the soil has been identified as clay having low plasticity (Figure 3).

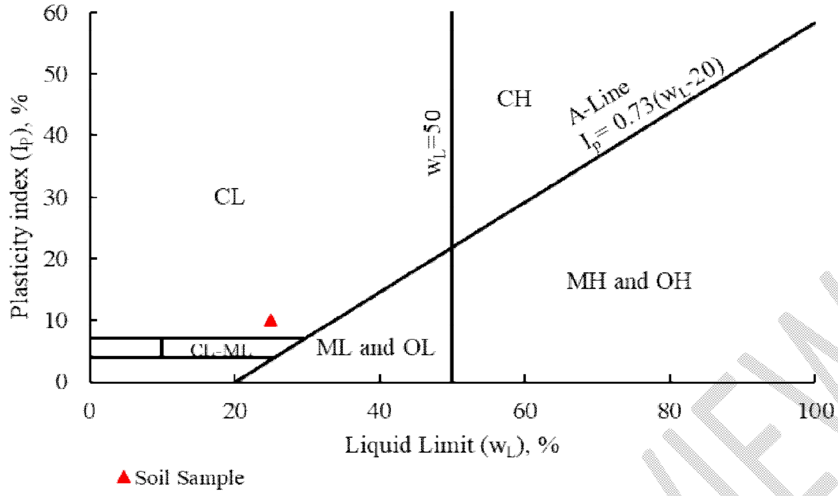

Figure 3: USCS classification of soil

4 ROCK MASS PARAMETERS

Vertical stress (σ_v) has been calculated by the equation 1.

$$\sigma_v = \gamma z \tag{1}$$

where, γ is unit weight of rock and z is overburden depth.

Horizontal stress (σ_h) is given by equation 2.

$$\sigma_h = k \gamma z + \sigma_{tec} \tag{2}$$

where, k = ratio of horizontal stress to vertical stress and σ_{tec} is tectonic stress. The tectonic stress for the SMHEP is 6 MPa in the north-south direction, and the resolving components of tectonic stress along and perpendicular to the cavern alignment leading to the headrace tunnel are 1.29 MPa and 5.93 MPa, respectively [9].

The horizontal-to-vertical stress ratio (k) is higher at a lesser depth due to the curvature of the earth [10], and the value is given by equation 3.

$$k = 0.25 + 7E\left(0.001 + \frac{1}{z}\right) \tag{3}$$

where E is the deformation modulus of earth crust in horizontal direction. According to Gautam [9], deformation modulus is taken as 3.97 GPa for banded gneiss. Values of k at different depths for banded gneiss are shown in Figure 4.

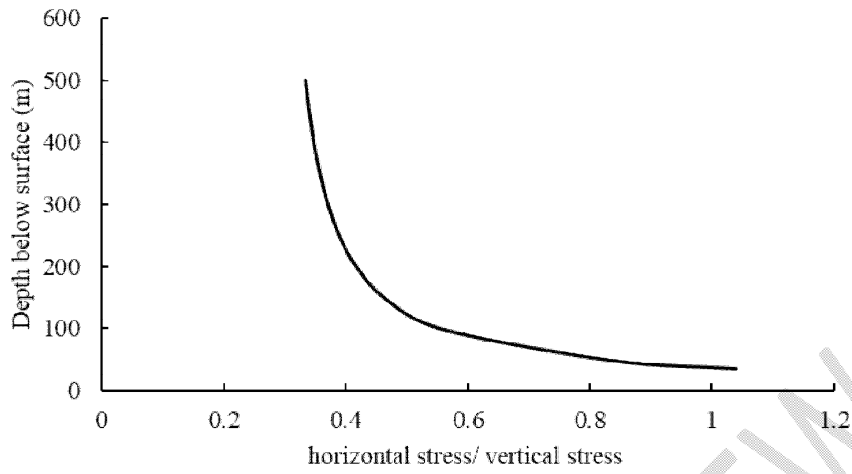

Figure 4: Variation of k with depth

Equations 4, 5 and 6 are used to calculate the Rock Mass Rating (RMR), Geological Strength Index (GSI) and deformation modulus of rock mass (E_{rm}) respectively. The intact strength of gneiss is taken as 130 MPa.

$$RMR = 15\log(Q) + 50 \quad (4)$$

$$GSI = RMR - 5 \quad (5)$$

$$E_{rm} = \left(1 - \frac{D}{2}\right) 10^{\frac{GSI-10}{40}} \quad (6)$$

The parameters of the rock mass on each of the study cross-sections have been provided in Table 1, while the parameters for numerical modeling are included in Table 2. For numerical modeling of rock, the disturbance factor is set to 0.8, while it is set to 0 for the part where soil predominates (Ch. 5+540 m).

Table 1: Rock mass parameters and rock mass classification for different chainages

Chainage (m)	Q	Q classification	RMR	RMR classification	GSI	E_{rm} (GPa)
1+000	0.344	Very poor rock	43	Fair rock	38	3.007
1+050	0.583	Very poor rock	46	Fair rock	41	3.574
1+100	0.229	Very poor rock	40	Poor rock	35	2.530
1+150	0.075	Extremely poor rock	33	Poor rock	28	1.691
1+200	0.038	Extremely poor rock	29	Poor rock	24	1.343
1+250	0.070	Extremely poor rock	33	Poor rock	28	1.691
1+300	1.250	Poor rock	51	Fair rock	46	4.766
1+350	1.083	Poor rock	51	Fair rock	46	4.766
1+400	0.271	Very poor rock	41	Fair rock	36	2.680
1+500	0.375	Very poor rock	44	Fair rock	39	3.185
3+600	0.500	Very poor rock	45	Fair rock	40	3.374
3+650	0.070	Extremely poor rock	33	Poor rock	28	1.691
3+700	0.038	Extremely poor rock	29	Poor rock	24	1.343

3+750	0.313	Very poor rock	42	Fair rock	37	2.839
3+800	0.344	Very poor rock	43	Fair rock	38	3.007
5+540	0.004	Exceptionally poor rock	14	Very poor rock	9	0.944

Table 2: Properties of rock and soil used for numerical modeling

Banded Gneiss		Clayey Soil	
Poisson's Ratio	0.2	Poisson's Ratio	0.4
Unit Weight (KN/m^3)	27	Unit Weight (KN/m^3)	18.673
Disturbance Factor	0.8	Cohesive Strength (MPa)	0.096
Material Constant (m_i)	28	Friction Angle (Degree)	35
Failure Criteria	Generalized Hoek-Brown	Failure Criteria	Mohr-Coulomb

The difference between the height of the original ground level and the elevation of the tunnel's top level was used to calculate the overburden values. Figure 5 depicts the variation in overburden values along the alignment. The overburden value is zero at the location of the Kalbandi river crossing, where water is piped from one side to the other and then released back into the tunnel.

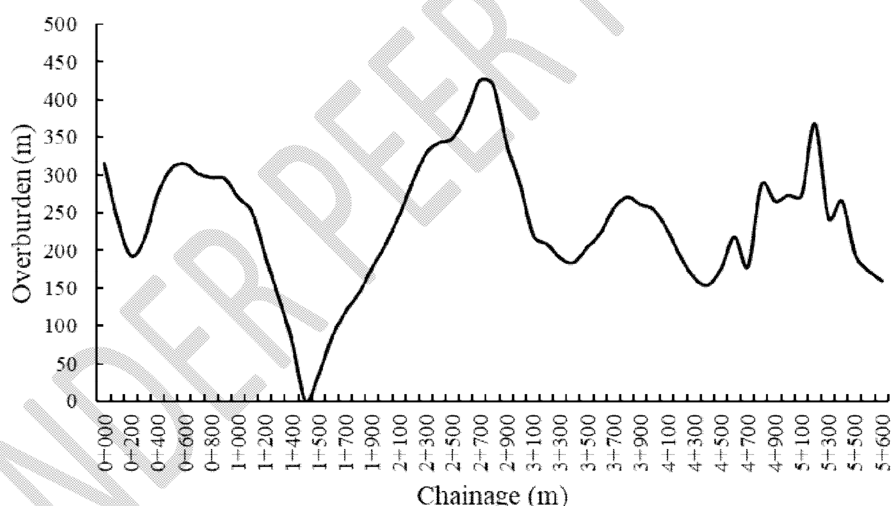

Figure 5: Overburden along the tunnel alignment

5 RESULT AND DISCUSSION

5.1 Squeezing Analysis

Squeezing ground conditions are a serious problem that can develop during excavation and last for a very long time. The Chameliya Hydroelectric Project headrace tunnel [11], the Modi Khola pressure tunnel, and the Kaligandaki headrace tunnel [12] are just a few of the Himalayan tunnels where this issue has been noted. As a result, it is crucial to investigate the tunnel hazards associated with squeezing in the area.

There are a number of techniques, including empirical, semi-empirical, and semi-analytical approaches, to forecast the possibility of squeezing. The Hoek and Marinos technique is regarded as the most trustworthy of them since it takes into account how the installation of supports affects tunnel strain.

The findings of the squeezing analysis in study section 1 are presented in Figure 6. The results indicate that there are no squeezing conditions present, as the strain is less than one percent in all sections.

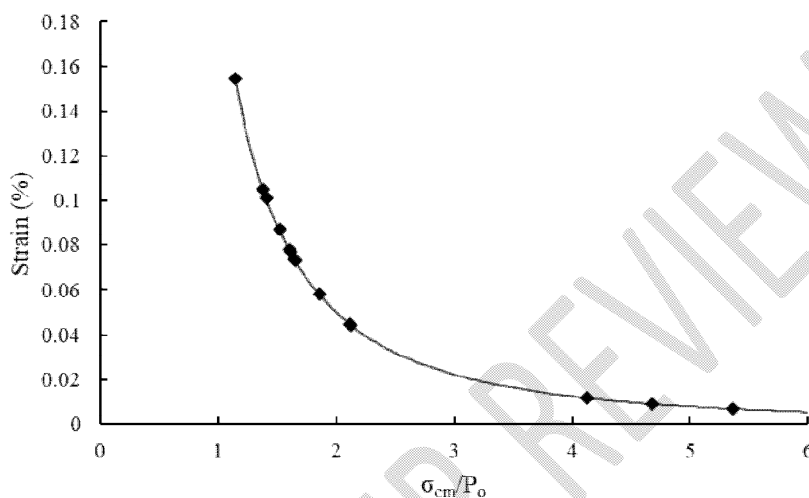

Figure 6: Tunnel strain vs σ_{cm}/P_0

5.2 Support estimation by empirical methods

Empirical methods are based on rock mass rating (RMR) and rock mass quality (Q) values of rock. There is a recommended set of standard tunnel supports for specific values of RMR or Q. Tables 3 and 4 present estimates of the supports based on Q and RMR values, respectively, for the study areas.

Table 3: Tunnel supports calculated from Q method

Support Category	Description
4	Unreinforced shotcrete of thickness 40 to 100 mm and 2.4 m long bolts at 1.6 m spacing
5	Fiber reinforced shotcrete of thickness 50 to 90 mm and 2.4 m long bolt at 1.4 m spacing
7	Fiber reinforced shotcrete of thickness 120 to 150 mm and 2.6 m long bolt at 1.2 m spacing

The Q chart suggests three types of supports for the rock formations in study section 1. The stability of the sections with poor quality rock at Ch. 1+300 m and Ch. 1+350 m does not require any support. However, Ch. 1+050 m needs category 4 support, while chainages 1+000 m, 1+100 m, 1+400 m, 1+500 m, 3+600 m, 3+750 m and 3+800 m need category 5 support. Additionally, chainages ranging from 1+150 m to 1+250 m and 3+650 m to 3+700 m necessitate support of category 7.

According to the RMR chart, supports are recommended in terms of the types of rocks present. Since there are fair and poor rock types in study section 1, the two types of support systems required are as given in Table 4.

Table 4: Tunnel supports calculated from RMR method

RMR	Rock Type	Supports
41-60	Fair	50 to 100 mm thick shotcrete in crown, 30 mm thick shotcrete in sides, 4 m long bolts at 1.5 to 2m spacing, wire mesh in crown
21-40	Poor	100 to 150 mm thick shotcrete in crown, 100 mm thick shotcrete in sides, 4 to 5 m long bolts at 1 to 1.5 m spacing with wire mesh, light to medium steel ribs at 1.5 m spacing

5.3 Numerical Modeling

Numerical modeling is done to evaluate the support needs for both static and seismic loading because the Q and RMR methods only estimate tunnel support requirements for static situations. Numerical modeling has been performed in Phase 2.0, a software for finite element analysis of excavations. The rock mass is modeled in two dimensions, considering that the tunnel is infinitely long. Chainages from study section 1 are modeled as rock and those from study section 2 are modeled as soil. The extent of external boundary is taken as four times of the tunnel diameter. Discretization is done with a six-noded triangle and the gradation factor is taken as 0.1. Figure 7 shows a representation of the 2D model.

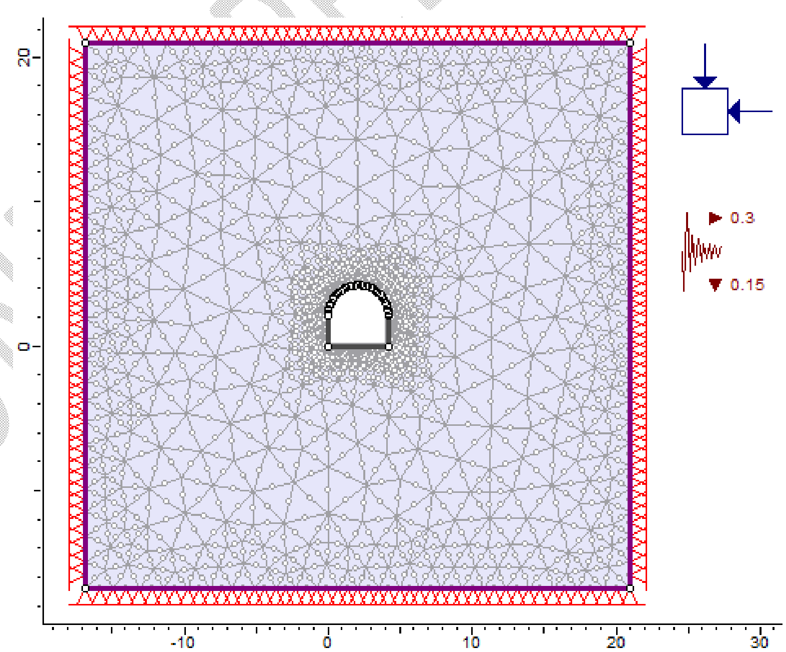

Figure 7: Finite element model showing mesh setup, static load and seismic load

For the analysis of tunnels in the Lesser Himalayas for various rock masses, horizontal seismic coefficient of 0.3 and vertical seismic coefficient of -0.15 are used [1] because maximum damage is observed in tunnels when peak horizontal acceleration is near 0.3g [13, 14] and maximum stresses are created on the tunnel perimeter when vertical seismic coefficient is acting downward [4]. For seismic analysis of tunnels, it is preferable to use vertical seismic coefficient as half of the horizontal seismic coefficient to account for the phase-lag between the horizontal and vertical peak ground acceleration [15].

The supports, obtained from empirical methods, have been modified with the help of finite element modeling in such a way that the final support system is both optimal and earthquake-resistant. The properties of shotcrete, rockbolt and steel rib used in the analysis are given in Table 5.

Table 5: Properties of liners used for numerical modeling

Shotcrete	
Compressive Strength	40 MPa
Beam Formulation	Timoshenko
Poisson's Ratio	0.25
Rockbolt	
Bolt Type	End Anchored
Diameter	20 mm
Bolt Modulus	200000 MPa
Tensile Capacity	0.1 MN
Steel Rib	
Grade	Fe 500

The plots showing support capacity depict the factor of safety of the liner elements for different rock types. Those liner elements that lie within a specific envelope are deemed safe for the given factor of safety. These plots are valuable not only for ensuring secure designs, but also for optimizing the support systems. Achieving a suitable factor of safety often necessitates several attempts, since empirical support approaches can result in either excessively safe or unsafe support systems. These plots represent the relationship between Thrust vs Shear and Thrust vs Moment, with each liner element being evaluated for failure in shear or moment. Once the elements fall within the envelope, the section is deemed safe for that factor of safety. The support systems that fulfill the safety requirements for seismic resistance are presented in Table 6 and the support capacity plots are shown from Figure 8 to 12. All the designed supports have the factor of safety of 1.5.

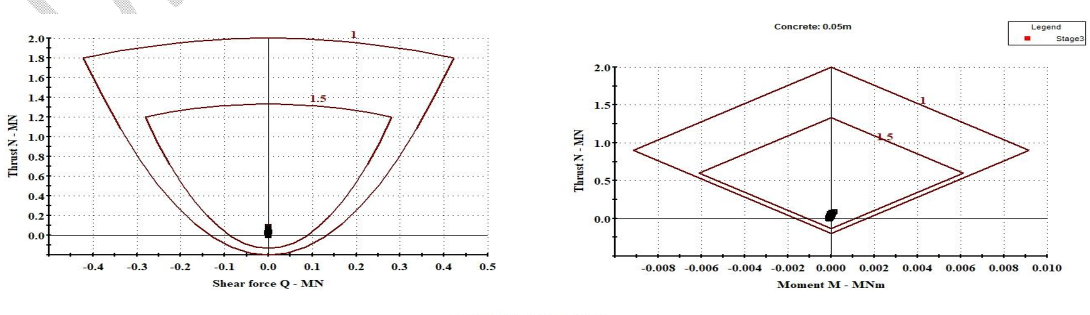

Figure 8: Support capacity plot at chainage 1+300 m (poor rock)

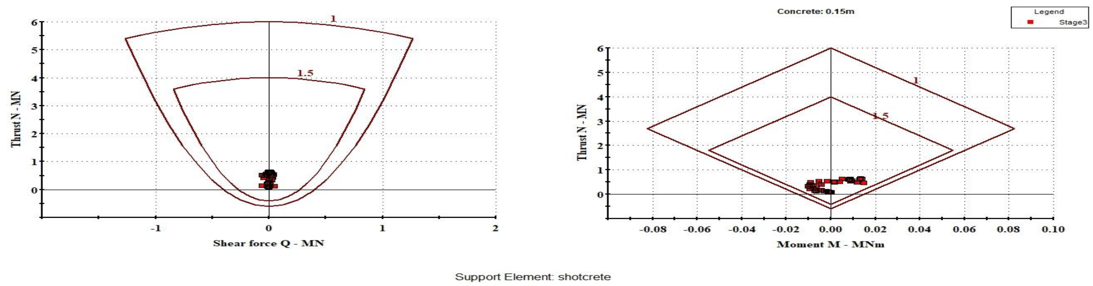

Figure 9: Support capacity plot at chainage 3+800 m (very poor rock)

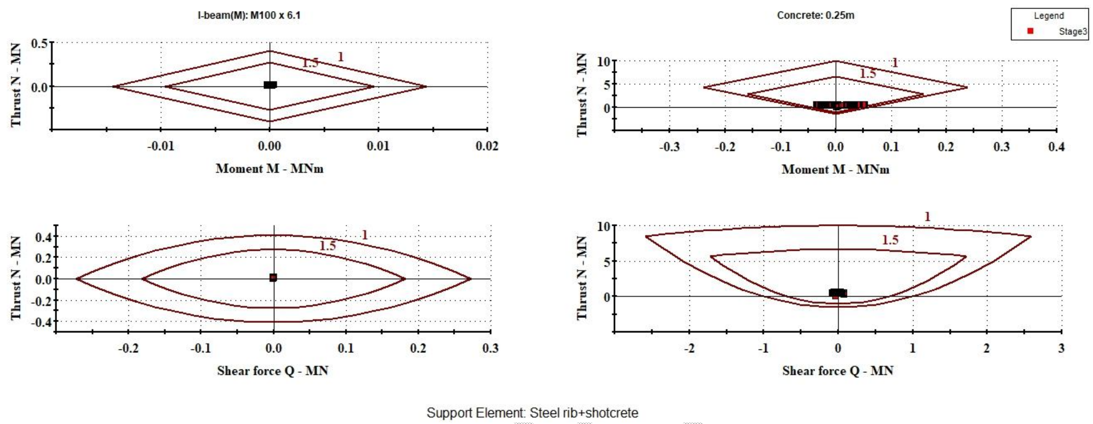

Figure 10: Support capacity plot at chainage 1+200 m (extremely poor rock)

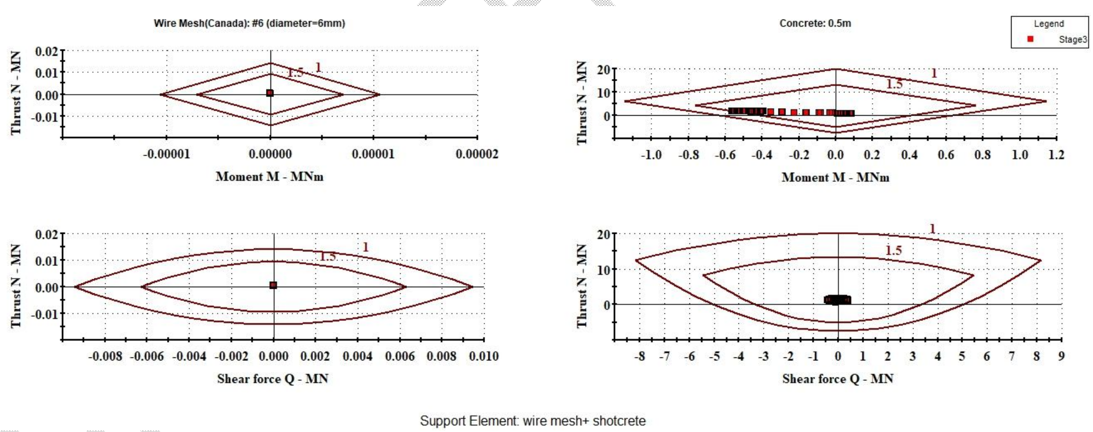

Figure 11: Support capacity plot of wire mesh and shotcrete at chainage 5+540 m (soft soil)

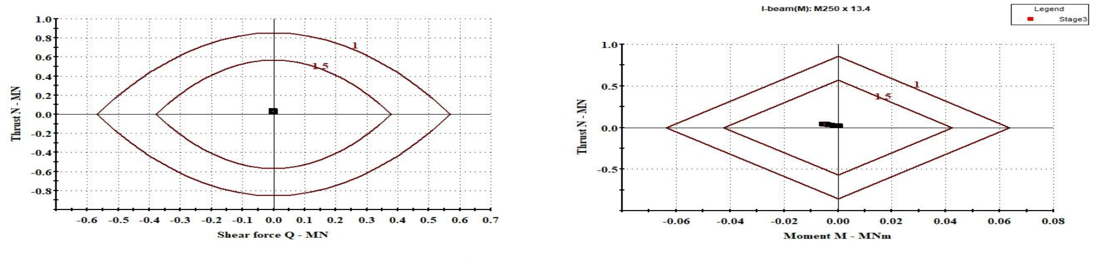

Figure 12: Support capacity plot of steel rib at chainage 5+540 m (soft soil)

Table 6: Final earthquake resistant supports for different geological conditions

Rock Type	Q value	Supports
Poor	1-4	Fiber reinforced shotcrete of 50 mm thickness, 1.5 m long rockbolt at 1.5×1.5 m spacing
Very Poor	0.1-1	Fiber reinforced shotcrete of 150 mm thickness, 1.5 m long rockbolt at 1.5×1.5 m spacing
Extremely Poor	0.01-0.1	Fiber reinforced shotcrete of 250 mm thickness, 2 m long rockbolt at 1.5×1.5 m spacing, M100×6.1 steel rib at 1 m spacing
Soft Soil	-	6 mm diameter wire mesh with 200 mm spacing filled with 500 mm thick fiber reinforced shotcrete, M250×13.4 steel rib at 0.5 m spacing

6 CONCLUSION

The study is focused on selecting a set of earthquake-resistant supports for each rock type in a Himalayan tunnel. Both empirical and finite element methods have been used for this. Horizontal and vertical seismic coefficients were taken as 0.3 and -0.15 respectively. Among all of these methods, numerical modeling has been found to not only provide safe support for the input magnitude of an earthquake load but also an optimized design with the help of support capacity plots. Therefore, numerical modeling is the only method to ensure both earthquake resistance and optimization of support requirements, which can function for any level of seismic load depending upon the seismicity of the project area. Using the Hoek and Marinos method, strain in the study section 1 has been found to be very insignificant. This shows a very low chance of the occurrence of the squeezing phenomenon.

REFERENCES

[1] S. Sapkota and G. B. Motra, “Seismic Impacts on Tunnels in Different Rock Mass,” in *Proceedings of 10th IOE Graduate Conference*, Oct. 2021, pp. 61–67.

[2] Y. M. A. Hashash, J. J. Hook, B. Schmidt, and J. I-Chiang Yao, “Seismic design and analysis of underground structures,” *Tunnelling and Underground Space Technology*, vol. 16, no. 4, pp. 247–293, Oct. 2001, doi: 10.1016/S0886-7798(01)00051-7.

[3] J.-N. Wang and G. A. Munfakh, “Seismic Design Of Tunnels,” *WIT Transactions on the Built Environment*, vol. 57, 2001.

[4] T. K. Sivarajan, “Seismic load considerations in the design of underground structures for hydropower projects in the Himalayan region,” in *Proceedings of the conference on Recent Advances in Rock Engineering (RARE 2016)*, Paris, France: Atlantis Press, 2016. doi: 10.2991/rare-16.2016.54.

[5] X. Zhang, Y. Jiang, and K. Maegawa, “Mountain tunnel under earthquake force: A review of possible causes of damages and restoration methods,” *Journal of Rock Mechanics and Geotechnical Engineering*, vol. 12, no. 2, pp. 414–426, Apr. 2020, doi: 10.1016/j.jrmge.2019.11.002.

[6] R. Shrestha, X. Li, L. Yi, and A. K. Mandal, “Seismic Damage and Possible Influencing Factors of the Damages in the Melamchi Tunnel in Nepal Due to Gorkha Earthquake 2015,” *Geotechnical and Geological Engineering*, vol. 38, no. 5, pp. 5295–5308, Oct. 2020, doi: 10.1007/s10706-020-01364-9.

[7] S. C. Sunuwar, “Nepal Earthquake 25 April 2015: Hydro projects damaged, risks and lessons learned for design considerations,” *Journal of Nepal Geological Society*, vol. 55, no. 1, pp. 141–149, Jun. 2018, doi: 10.3126/jngs.v55i1.22804.

[8] D. R. Joshi, S. Panthee, and B. N. Ghimire, “Numerical Modeling for Engineering Analysis and Designing of Rock Support for Headrace Tunnel,” *International Research Journal of Engineering and Technology*, 2021, [Online]. Available: www.irjet.net

[9] U. Gautam, “Stability Assessment of the Underground Settling Basin Cavern of Super Madi Hydroelectric Project, Nepal,” Master Thesis, Norwegian University of Science and Technology, Trondheim, 2012.

[10] P. R. Sheorey, “A theory for In Situ stresses in isotropic and transverseley isotropic rock,” *International Journal of Rock Mechanics and Mining Sciences & Geomechanics Abstracts*, vol. 31, no. 1, pp. 23–34, Feb. 1994, doi: 10.1016/0148-9062(94)92312-4.

[11] P. K. Shrestha, K. K. Panthi, and C. B. Basnet, “Analysis of Squeezing Phenomenon in the Headrace Tunnel of Chameliya Project, Nepal,” *Hydro Nepal: Journal of Water, Energy and Environment*, vol. 13, pp. 44–51, Mar. 2014, doi: 10.3126/hn.v13i0.10039.

[12] K. K. Panthi, “Analysis of Engineering Geological Uncertainties Related to Tunnelling in Himalayan Rock Mass Conditions,” PhD Thesis, Norwegian University of Science and Technology, Trondheim, 2006.

[13] S. Sharma and W. R. Judd, “Underground opening damage from earthquakes,” *Eng Geol*, vol. 30, no. 3–4, pp. 263–276, Jun. 1991, doi: 10.1016/0013-7952(91)90063-Q.

[14] N. Roy and R. Sarkar, “A Review of Seismic Damage of Mountain Tunnels and Probable Failure Mechanisms,” *Geotechnical and Geological Engineering*, vol. 35, no. 1, pp. 1–28, Feb. 2017, doi: 10.1007/s10706-016-0091-x.

[15] T. Tshering, “The Impact of Earthquakes on Tunnels in different Rock Mass Quality Q: A numerical analysis,” Master Thesis, University of Oslo, Oslo, 2011.